JOINT WMO TECHNICAL PROGRESS REPORT ON THE GLOBAL DATA PROCESSING AND FORECASTING SYSTEM AND NUMERICAL WEATHER PREDICTION RESEARCH ACTIVITIES FOR 2016

Hong Kong Observatory, Hong Kong, China

1 Summary of highlights

(i) The WMO WWRP 4th International Symposium on Nowcasting and Very-short-range Forecast 2016 (WSN16), AvRDP training workshop, and two related WMO meetings were hosted in Hong Kong, China in July 2016. WSN16 was attended by over 160 participants from 26 countries/regions.

(ii) Following commencement of dropsonde reconnaissance for tropical cyclones over the northern part of the South China Sea by Hong Kong Observatory in late 2016, research was being carried out on the assimilation of dropsonde observations through variational and ensemble-based methods for improving TC track, intensity and structure forecasts.

(iii) The community version of the nowcasting system "Short-range Warning of Intense Rainstorms in Localized Systems (SWIRLS)" (Com-SWIRLS) was made available to NMHSs and a user website (http://swirls.hko.gov.hk/) was established. Technical support was provided to meteorological services in China (Shanghai, Zhuhai and Macao), India, Malaysia, Myanmar, the Philippines and South Africa. Training was provided to meteorologists from a dozen of countries.

(iv) Location-specific lightning nowcast, extended forecasts of temperatures for day 10-14, and tropical cyclone track probability forecast were developed and launched.

(v) A sub-kilometre resolution NWP suite, the Aviation Model (AVM), continued supporting detailed weather forecasts for the Hong Kong International Airport. The system hardware was enhanced in late 2016 in preparation for full domain coverage of the Hong Kong territory at an unprecedented 200-m resolution.

(vi) A mesoscale ensemble prediction system (MEPS) at 10-km resolution continued to support in-house probabilistic assessment of high-impact weather, with notable performance in a number of tropical cyclone and rainstorm cases. Advanced ensemble-based assimilation algorithms were being developed for ingestion of new remote-sensing data e.g. large-area radar composites and Himawari-8 cloudy radiance.

2 Equipment in use

Machine	Quantity	Peak performance	No. of CPU	Memory	Year of Installation
IBM S814 Server	1	66.9 GFLOPS	4	16 GB	2016
Dell R720 Cluster	1	3.0 TFLOPS (CPU) 9.4 TFLOPS (GPU)	18 CPU 8 GPU	1,728 GB (CPU) 40 GB (GPU)	2014
Dell HPC Cluster	1	18.7 TFLOPS	119	3,504 GB	2013
Dell HPC Cluster	1	19.6 TFLOPS	134	4,288 GB	2013/2016
HP Cluster	1	1.8 TFLOPS (CPU) 15.2 TFLOPS (GPU)	16 CPU 21 GPU	1,056 GB (CPU) 120 GB (GPU)	2012-14
Dell R510 Server	1	68.0 GFLOPS	8	12 GB	2012

IBM BladeCenter JS23	1	64.0 GFLOPS	4	16 GB	2012
Dell R710 Cluster	1	1.3 TFLOPS	16	384 GB	2011
Dell HPC Cluster	1	7.7 TFLOPS	186	2,120 GB	2010
IBM BladeCenter JS22	1	64.0 GFLOPS	4	12 GB	2009
IBM p630 Cluster	1	48.0 GFLOPS	12	28 GB	2004
IBM SP Cluster	1	36.0 GFLOPS	24	13.5 GB	2001

The GTS data management system originally running on IBM BladeCenter JS22 server was migrated to an IBM S814 server in February 2016. The JS22 server was redeployed for other operational and R&D activities.

An HPC system with 37 computational nodes and an aggregated peak performance of 12 TFLOPS continued to support HKO's high-resolution Aviation Model (AVM) for fine-scale forecasts around the Hong Kong International Airport (HKIA). The cluster was expanded in late 2016 to provide a total aggregated peak performance of 19.6 TFLOPS in preparation for the computational requirement for extending the domain to cover the whole territory.

3 Data and Products from GTS in use

The approximate number of bulletins of observations received from GTS (in both alphanumeric and BUFR messages) on a typical day in 2016 is given below:

	Alphanumeric	BUFR
SYNOP/SHIP/BUOY	25,000	7,300
Radiosonde (TEMP/PILOT)	1,100	750
AIREP	450	--
AMDAR	1,700	4,100
SATEM/SATOB	200	750
ATOVS	--	3,500
Scatterometer wind (ASCAT)	--	14,000
Wind Profiler	--	250
Drifting Buoy	3,400	--

Other observations and reports, such as RADOB, SAREP and DROPSONDE were also gathered through the GTS during the passage of tropical cyclones.

The approximate number of bulletins or files of NWP products received from GTS on a typical day in 2016 is given below:

Centre	Type	Number
China Meteorological Administration (CMA)	GRIB	130*
Deutscher Wetterdienst (DWD)	GRIB	1,900
European Centre for Medium Range Weather Forecasts (ECMWF)	GRIB	6,000
Japan Meteorological Agency (JMA)	GRIB	9,200
United Kingdom Meteorological Office (UKMO)	GRIB	2,600

*CMA NWP products are grouped by forecast hour and comprise multiple forecast elements.

NWP products from the US National Centers for Environmental Prediction (NCEP), ECMWF, JMA, Korea Meteorological Administration (KMA) and Canadian Meteorological Centre (CMC) are also acquired through the Internet.

4 Forecasting system

4.1 System run schedule and forecast ranges

4.1.1 AIR/NHM

The Atmospheric Integrated Rapid-cycle (AIR) forecast model system is operated in two forecast domains with horizontal resolution at 10 km and 2 km (Wong, 2011) using the Non-Hydrostatic Model (NHM) developed by the Japan Meteorological Agency (JMA) (Saito et al. 2006).

The outer 10-km resolution model, named as Meso-NHM, is run 8 times a day to generate 72-hour forecasts. The map projection of the model is Lambert Conformal Conic with the lower left corner at 0.91^{o}N, 84.42^{o}E and the upper right corner at 37.48^{o}N, 168.13^{o}E. The initial condition is based on the 3-dimensional variational data assimilation (3DVAR) analysis at 00, 03, 06, 09, 12, 15, 18 and 21 UTC with observation cut-off time of about 2.5 hours. The boundary conditions are extracted from the ECMWF Integrated Forecast System (IFS) forecasts. Additional Meso-NHM runs using GSM forecasts from JMA are conducted at 00 and 12 UTC with a view to capturing various scenarios on the development of synoptic and mesoscale systems under different model boundary conditions.

The inner 2-km resolution model, known as RAPIDS-NHM, is run on an hourly basis covering an area 19.5 – 25.0 °N, 111.2 – 117.1 °E with forecast range of 15 hours. The initial condition is obtained from the 3DVAR analysis at 00, 01, …, 23 UTC with observation cut-off time of about 35 minutes, and the boundary conditions are prescribed by Meso-NHM forecasts.

4.1.2 Aviation Model (AVM)

The AVM is a high-resolution implementation of the Weather Research and Forecast (WRF) model (Skamarock, 2008) in support of fine-scale aviation weather forecasts for the HKIA.

AVM is operated in two single-nested forecast domains with horizontal resolution of 600 m and 200 m, covering respectively the Pearl River Estuary region (AVM-PRD) and the immediate vicinity of the HKIA (AVM-HKA). The outer domain covers an area of about 350 km × 350 km (20.8 – 23.8 °N, 112.2 – 115.6 °E) while the inner domain covers about 50 km × 50 km (22.08 – 22.53 °N, 113.68 – 114.16 °E). In late 2016, following hardware expansion of the AVM-HPC, the inner AVM domain (“AVM-xHKA”) was extended to provide full coverage of the Hong Kong territory (about 110 km x 110 km, 22.0 – 22.8 °N, 113.7 – 114.5 °E).

Forecasts of both domains are updated at hourly intervals and originally cover up to T+7 hours. Following hardware upgrade, the AVM-PRD and AVM-HKA runs are extended to T+9. It is expected that the AVM-xHKA runs, when available, will follow an optimised schedule alternating between T+12 and T+3 to provide extra temporal coverage for the HKIA. Initial conditions are obtained from 3D-VAR analysis performed hourly with

observation cut-off time of about 15 minutes. Boundary conditions, as well as first guesses for 3D-VAR analysis, for AVM-PRD and AVM-HKA are based on the latest available output from RAPIDS-NHM and the concurrent forecast of AVM-PRD respectively.

4.2 Medium range forecasting system (4-10 days)

For public consumption, HKO routinely issues two types of medium-range forecast products out to 9 days ahead on Internet website, namely the "9-day Weather Forecast" formulated by forecasters and the computer-generated "Automatic Regional Weather Forecast in Hong Kong & Pearl River Delta Region" (ARWF).

The "9-day Weather Forecast" is formulated primarily based on forecasters' subjective assessment of observations and various prognostic forecast products from the global models of ECMWF, JMA, NCEP, CMA, KMA and UKMO as well as HKO's Meso-NHM. Forecast of various meteorological elements are presented to forecasters in various formats, including weather maps, time series, time cross-section, forecast tephigrams, etc. References are also made to other forecast products from the EPSs of ECMWF, JMA and KMA for assessment of the confidence and uncertainty involved.

The ARWF webpage (http://maps.weather.gov.hk/ocf/index_e.html) presents the objective station-specific forecasts and gridded forecasts over Hong Kong and the Pearl River Estuary regions using a web-based geographic information system (GIS). Forecast elements include temperature, relative humidity, wind direction and wind speed, daily chance of rain over Hong Kong, and weather forecast icons. Such forecasts are automatically updated twice a day up to nine days ahead based on the Objective Consensus Forecast methodology.

4.2.1 Operational techniques for application of NWP products (MOS, PPM, KP, Expert Systems, etc.)

4.2.1.1 In operation

4.2.1.1.1 Tropical Cyclone Information Processing System (TIPS)

The Tropical Cyclone Information Processing System (TIPS) has been in operation since 2005, integrating various information for use by forecasters in the preparation of tropical cyclone forecasts and warnings, including a) NWP products from Meso-NHM operated by HKO (see Section 4.3 below), global models of ECMWF, JMA, UKMO, NCEP, CMA, KMA and CMC, as well as the Hurricane Weather Research and Forecast (HWRF) modelling system of NCEP; b) subjective forecasts and warning from meteorological centres; and c) satellite and radar fixes and imageries from meteorological centres. TIPS can generate ensemble tracks up to 9 days ahead from model forecasts for reference by the forecasters. In addition to position-based consensus method, a motion vector consensus method was available in TIPS to handle incomplete model forecasts in generating ensemble TC tracks. Ensemble mean tracks and TC strike probability information derived from the EPS forecast data of various centres were also available to facilitate the construction of warning tracks.

4.2.1.1.2 Objective Consensus Forecast (OCF)

Following the work of Engel and Ebert (2007), a system called the Objective Consensus Forecast (OCF) has been developed. Forecast time-series of temperature, daily minimum

and maximum temperatures, wind speed and wind direction, dew point, relative humidity, weather icon (describing the state of sky and rainfall) and daily probability of precipitation for various locations in Hong Kong up to 384 hours (since 2016) ahead can be generated based on an ensemble of post-processed outputs from Meso-NHM, global deterministic model forecasts from ECMWF, JMA, NCEP, CMA and UKMO (included in 2016), as well as EPS from ECMWF. Time-lagged ensembles of the maximum and minimum temperature forecasts from OCF are also made available to facilitate forecasters' assessment on the regional temperatures over Hong Kong in the following 9 days.

In 2016, wet-bulb temperature forecast was introduced to the forecast suite of OCF. A tool for customising the time series was made available to facilitate preparing the graphics on model temperature forecasts for TV presentation.

4.2.1.1.3 Automatic Weather Forecast

Automatic Weather Forecast system provides worded/iconified objective forecast guidance on local winds, state of sky, weather, temperature and relative humidity up to 9 days ahead for reference by forecasters. It runs twice a day based primarily on 00- and 12-UTC outputs from ECMWF, JMA, NCEP, Meso-NHM, as well as some local forecasting rules. Besides, probabilities of precipitation for each day are computed based on the output of ECMWF EPS. In addition to the use of direct model output, key post-processing techniques employed in the system include linear regression, Kalman–filtering, logistic regression and poor-man's ensemble averaging.

4.2.1.1.4 Analogue Forecast System

In support of forecaster's rainfall forecast, an Analogue Forecast System is run based on ECMWF's ERA Interim re-analysis data since 1979 with special focus put on capturing the heavy rainfall events in the vicinity of Hong Kong. It outperformed the direct model outputs in forecasting heavy rainfall events by being able to capture their occurrences at a higher detection rate and lower false alarm ratio. The forecast guidance is provided in terms of daily rainfall category out to 7 days ahead. It is updated once a day based on the 12-UTC run of ECMWF data.

4.2.1.1.5 Tropical Cyclone Forecast Guidance

The EPS tropical cyclone (TC) forecast product suite provides various plots of ensemble tracks and strike probability maps (SPM) based on individual global EPSs, namely ECMWF, NCEP, EGRR, JMA, JMA TEPS, CMC, CMA, KMA, as well as two grand ensembles (i.e., ECMWF + NCEP + EGRR and ECMWF + NCEP + EGRR + JMA TEPS). The SPMs represent forecast TC positions up to 120 hours. In 2016, an interactive webpage was introduced to generate TC products from the ECMWF ensemble tracks during pre-genesis stage.

The statistical-dynamical TC intensity forecast (TINT) guidance makes use of relationships between the HKO best track data and ECMWF's ERA Interim re-analysis to provide TC intensity forecasts. In 2016, a new module of TINT, called TINT-RI, was introduced to provide guidance on rapid intensification using 200hPa divergence, 300-500hPa RH, 200-850 hPa vertical windshear (from ECMWF reanalysis) and heat potential (from NOAA) as predictors. Moreover, a new web portal was launched for an integrated display of all TC intensity forecast guidance, including intensity forecasts from warning centres, NWP models,

TINT, TINT-RI, as well as other numerical guidance from JTWC including HWRF and SHIPS. Verification for TCs in 2016 showed that TINT-RI outperformed global NWPs, demonstrated higher skill than HWRF and was comparable to the skill of HKO subjective warnings.

4.2.2 Ensemble Prediction System (EPS)

Meteograms from the EPS of ECMWF, JMA and KMA for the grid points in the vicinity of Hong Kong are generated for forecasters' reference. Other ECMWF EPS products, such as Extreme Forecast Index (EFI), Shift of Tails (SOT), probability of precipitation, probability of high winds, spaghetti diagrams and stamp maps of MSLP and geopotential height at 500hPa level, are also available.

An in-house mesoscale ensemble prediction system (MEPS) provides twice-daily (initialised at 00 UTC and 12 UTC) 20-member forecasts up to T+72 for the southern China and western North Pacific region. Post-processed products available in real-time include stamp maps, probabilities of various high-impact weather (including precipitation, high winds, extreme temperatures, instability indices, etc.) as well as tropical cyclone strike probability.

4.3 Short-range forecasting system (0-72 hrs)

4.3.1 Data assimilation, objective analysis and initialization

4.3.1.1 In operation

4.3.1.1.1 AIR/NHM

Meteorological data assimilated by the 3-dimensional variational data assimilation system (3DVAR) of AIR/NHM are as follows:

(A) <u>From GTS</u>

SYNOP, BUOY, SHIP	surface and ship data
TEMP, PILOT	radiosonde and pilot data
AMDAR and AIREP	aircraft data
ATOVS	retrieved temperature profile from polar-orbiting satellites
AMV	atmospheric motion vector from HIMAWARI-8
Ocean surface wind	scatterometer wind retrieval data from ASCAT/RapidScat/HY-2A
IASI	temperature and humidity retrieval profile data from EUMETSAT Metop IASI (Infrared Atmospheric Sounding Interferometer)

(B) <u>Through regional data exchange</u>
Data from automatic weather stations and weather radars in Guangdong

(C) <u>Local observations</u>
Automatic weather station data
Doppler weather radar data
Retrieved wind data from mosaic of weather radars in Hong Kong and Guangdong
Wind profiler data

Ground-based Global Positioning System (GPS) reception network

(D) From NCEP data server
Daily high resolution sea surface temperature (HR-SST) analysis at 0.083-degree resolution in latitude/longitude

Initial conditions of Meso-NHM and RAPIDS-NHM are generated using 3DVAR analysis running at full horizontal resolution and model vertical levels. The first guess of 3DVAR analysis in Meso-NHM is obtained from the ECMWF IFS/JMA GSM. In RAPIDS-NHM 3DVAR system, the Meso-NHM forecast is used as the background.

Total precipitable water vapour (PWV) retrieved from SSM/I is assimilated in Meso-NHM 3DVAR. To prescribe the sea-surface temperature field in Meso-NHM, SST analysis from ECMWF is used.

In RAPIDS-NHM, PWV from the local ground-based GPS stations and Doppler velocity data from the two weather radars in Hong Kong are assimilated in the 3DVAR analysis. 3-dimensional variational wind retrieval is applied to generate upper level wind data over Hong Kong and nearby regions using Doppler velocity and reflectivity data from the weather radars in Hong Kong and Guangdong. The retrieved wind data are used to support the monitoring and nowcast of severe weather, and they are ingested in RAPIDS-NHM 3DVAR as additional upper-air wind observations (Wong *et al.* 2011).

RAPIDS-NHM 3DVAR is used to provide the hourly mesoscale analysis of wind, temperature, relative humidity on surface and upper levels at full horizontal resolution (2 km). Diagnostic fields including instability indices, equivalent potential temperature, moisture transport and moisture flux convergence are generated for forecasters' reference on analysis of mesoscale weather process and nowcasting of severe weather systems.

4.3.1.1.2 AVM

Meteorological data assimilated by the 3-dimensional variational data assimilation system (3DVAR) of AVM are as follows:

(A) From GTS

SYNOP, BUOY, SHIP	surface and ship data
TEMP, PILOT	radiosonde and pilot data
AMDAR and AIREP	aircraft data

(B) Local observations
Dense surface observations from the automatic weather station networks from Hong Kong and Guangdong, including weather buoys
Wind observations from wind profilers in Hong Kong
Temperature and humidity profiles from microwave radiometer

Initial conditions of AVM-PRD and AVM-HKA/AVM-xHKA are generated using 3D-VAR analysis running at full horizontal resolution and model vertical levels. The first guess of 3D-VAR analysis in AVM-PRD is based on the output from the latest available run of the 2-km RAPIDS-NHM, normally at a time lag of 1 – 2 hours. For AVM-HKA/AVM-xHKA, the background field is taken from the concurrent AVM-PRD output with outstanding forecast hours, if any, supplemented by Rapids-NHM.

4.3.1.2 Research performed in this field

4.3.1.2.1 Extended domain Meso-NHM

Research was carried out to study the impact of assimilating the clear sky radiance (CSR) from Himawari-8 into Meso-NHM. Some positive impact was observed. Experiments were also carried out to study the impact of replacing JNoVA-3DVAR with WRFDA-3DVAR on the forecast of Meso-NHM.

4.3.1.2.2 Extended domain AVM

Fine-tuning of data assimilation algorithm, surface and boundary layer physical processes were carried out throughout 2016 to improve performance in winds and temperature forecasts, particularly over the HKIA region and urban areas in Hong Kong.

Additionally, following the commencement of dropsonde reconnaissance for TCs over the northern part of the South China Sea by HKO in late 2016, research was being carried out on the assimilation of dropsonde observations through variational and ensemble-based methods (Chan et al 2017) with a view to improving forecasts of TC track, intensity and structure.

4.3.2 Model

4.3.2.1 In operation

4.3.2.1.1 AIR/NHM

Specification of Meso-NHM and RAPIDS-NHM in AIR forecast model system:

	Meso-NHM	**RAPIDS-NHM**
Horizontal resolution	10 km	2 km
Horizontal grid	Arakawa-C	
Map projection	Lambert Conformal Conic	Mercator
No. of grid points	841×515	305×305
Vertical coordinates	Terrain following height coordinates using Lorenz grid	
No. of vertical levels	50	60
Time step	30 s	8 s
Initial time	00, 03, 06,…, 21 UTC (for using ECMWF IFS forecast as boundary) 00 and 12 UTC (for using JMA GSM forecast as boundary)	Every hour
Forecast range	72 hours	15 hours

Initial condition	3DVAR using background from ECMWF IFS/JMA GSM forecast	3DVAR using background from Meso-NHM forecast
Boundary condition	ECMWF IFS forecast data (00 and 12 UTC) at 0.125 degree resolution in lat/lon Boundary data including: pressure, horizontal wind components (U and V), temperature (T) and relative humidity (RH) on surface; and U,V,T,RH and geopotential height at 21 pressure levels (1000,975,950,925,900,850,800, 700,600,500,400,300,250,200,150,100, 70, 50, 30, 20, 10 hPa) JMA GSM forecast data (00 and 12 UTC) at 0.5 degree resolution in lat/lon Boundary data including: pressure, horizontal wind components (U and V), temperature (T) and relative humidity (RH) on surface; and U,V,T,RH and geopotential height at 21 pressure levels (1000,975,950,925,900,850,800, 700,600,500,400,300,250,200,150,100, 70, 50, 30, 20, 10 hPa)	Meso-NHM forecast on 50 model levels
Nesting configuration	One-way nesting	
Topography	USGS GTOPO30 (30 second data smoothed to 1.5 times horizontal resolution) with modifications over Hong Kong areas based on USGS-SRTM (Shuttle Radar Topography Mission) dataset	
Land-use characteristics	USGS Global Land Cover Characterization (GLCC) 30 second data and 24 land-use types with modifications over Hong Kong	
Dynamics	Fully compressible non-hydrostatic governing equations solved by time-splitting horizontal-explicit-vertical-implicit (HEVI) scheme using 4^{th}-order centred finite differencing in flux form	
Cloud microphysics	3-ice bulk microphysics scheme	
Convective parameterization	Kain-Fritsch scheme (JMA version) (before 29 June 2016) / EC Tiedtke based scheme (HKO version) (Since 29 June 2016)	-
Surface process	Flux and bulk coefficients: Over land: Beljaars and Holtslag (1991), Donelan et al. (2004); Over sea: Beljaars and Holtslag (1991), Donelan et al. (2004)	

	(Meso-NHM before 29 June 2016 and RAPIDS-NHM); Wong et. al. (2011) (Meso-NHM since 29 June 2016) Roughness length: Beljaars (1995) and Fairall et al. (2003); Stomatal resistance and temporal change of wetness included; 4-layer soil model to predict ground temperature and surface heat flux.
Turbulence closure model and planetary boundary layer process	Mellor-Yamada-Nakanishi-Niino Level 3 (MYNN-3) (Meso-NHM before 29 June 2016 and RAPIDS-NHM) / Mellor-Yamada-Nakanishi-Niino Level 2.5 (MYNN-2.5) (Meso-NHM since 29 June 2016) (Nakanishi and Niino, 2004) with partial condensation scheme (PCS) and implicit vertical turbulent solver Height of PBL calculated from virtual potential temperature profile.
Atmospheric radiation	Long wave radiation process following Kitagawa (2000) Short wave radiation process using Yabu *et al.* (2005) Prognostic surface temperature included; Cloud fraction determined from PCS.

For further details on NHM and AIR forecast model system, please refer to Saito *et al.* (2006) and Wong (2011) respectively.

4.3.2.1.2 AVM

The characteristics of AVM are shown as follows:

	AVM-PRD	**AVM-HKA/AVM-xHKA**
Horizontal resolution	600 m	200 m
Horizontal grid	Arakawa-C	
Map projection	Mercator	
No. of grid points	581×581	253×253 / 581×581
Vertical coordinates	Terrain-following eta coordinates	
No. of vertical levels	42	42 / 60
Initial time	Every hour	
Forecast range	7 - 9 hours	3 - 12 hours
Initial condition	3D-Var using background from RAPIDS-NHM forecast	3D-Var using background from AVM-PRD forecast
Boundary condition	Latest available RAPIDS-NHM forecast interpolated onto 42 pressure levels	Concurrent AVM-PRD forecast on full model levels
Nesting configuration	One-way nesting	
Topography	USGS GTOPO30 (30 second data) with local adaptations	
Land-use characteristics	USGS Global Land Cover Characterization (GLCC) 30 second data and 24 land-use types with local adaptations	
Dynamics	Fully compressible non-hydrostatic governing equations in flux form	
Cloud microphysics	WRF double-moment 6-class scheme	

Convective parameterization	-
Surface processes and boundary layer	Noah LSM; LES PBL scheme with local adaptations
Atmospheric radiation	Longwave radiation: RRTMG scheme Shortwave radiation: RRTMG shortwave scheme

Please refer to Skamarock (2008) for technical details of the Weather Research and Forecast (WRF) Model (Version 3.7.1).

4.3.2.2 Research performed in this field

In the current configuration of AVM, the inner AVM-HKA domain, which is centred around HKIA, covers only the southwestern portion of Hong Kong. With a view to better supporting detailed regional weather forecasts as well as aviation applications, the AVM-HKA domain would be extended to provide full coverage of Hong Kong territory at 200-m resolution. Forecasts experiments using the extended domain indicated small but positive benefits in surface temperature and upper-air wind forecasts by verification against AWS and aircraft observations.

4.3.3 Operationally available NWP products

4.3.3.1 AIR/NHM

For Meso-NHM, 3-hourly prognostic charts on surface (3-hour accumulated rainfall, mean sea level pressure, temperature, relative humidity, wind, CAPE) and upper levels (925, 850, 700, 500 and 200 hPa for elements including geopotential height, wind, relative humidity, divergence, relative vorticity), time series, time cross section, vertical cross section and tephigram for grid points at strategic locations in Hong Kong are generated every 3 hours. For RAPIDS-NHM, similar products are generated but at hourly intervals and hourly output frequency. In addition, simulated radar reflectivity products such as maximum reflectivity, reflectivity at 3 km altitude, isothermal reflectivity at -10°C and vertically integrated ice content; as well as the mesoscale diagnostic products including moisture transport, moisture flux convergence and updraft helicity for RAPIDS-NHM are routinely generated for forecasters' reference in significant convection forecasting.

4.3.3.2 AVM

Routinely available products from AVM-PRD include prognostic charts of upper-air (wind, humidity, divergence and vorticity) and surface elements (pressure, temperature, dew point and relative humidity) at hourly intervals. Upper-air charts are provided at standard pressure levels of 925, 850, 700, 500 and 200 hPa.

In addition to forecast rainfall accumulated at hourly intervals, a suite of mesoscale diagnostic parameters (including CAPE, K-Index, vertical windshear and storm-relative helicity) are developed in support of short-term forecasts of severe convection. Specialised products for aviation applications are mentioned in Section 4.3.4.1. Simulated 3-km radar reflectivity images are also routinely generated to provide guidance on mode of convection.

4.3.3.3 Products for other meteorological services

TC track forecast guidance from Meso-NHM is routinely generated and disseminated via GTS. The guidance is issued and updated twice a day based on the 00 and 12 UTC model runs whenever a TC reaching tropical depression strength occurs in the area of responsibility of HKO (10 – 30 ^{o} N, 105 – 125 ^{o}E). The information provided in the guidance includes forecast TC positions and intensity changes at 6-hourly intervals up to 72 hours ahead. TC warning position and intensity analysed by HKO at 00 and 12 UTC are also included as initial values.

Up to the end of 2016, HKO is providing city-specific forecast times series and time cross sections for a total of 188 cities (15 cities of Tajikistan added in 2016) of the RA II Members under the RA II Project on City-Specific NWP Products, via a password-protected web site maintained by HKO. The products are generated using the direct model output from Meso-NHM. Table 4.3.3.1 summarised the forecast elements provided in the RA II project.

Table 4.3.3.1 Forecast of meteorological elements provided in the RAII project on City-Specific NWP Products

Content	Levels	Initial Time	Forecast Hours	Display Format
Sea level pressure	Sea level	00 and 12 UTC	3-hourly intervals from 3 to 72 hours	Graphical and tabulated data formats
3-hourly precipitation	Surface			
Surface relative humidity	Surface			
Total cloud amount	-			
Air temperature	Surface, 925, 850, 700, 600, 500, 400, 300, 250, 200, 150 and 100 hPa			
Dew point temperature				
Wind speed and direction				
Geopotential height	500 hPa			

Selected model products derived from Meso-NHM are also disseminated in graphical format via the Internet (Table 4.3.3.2) for public consumption (URL: http://www.weather.gov.hk /nhm/nhme.htm).

Table 4.3.3.2 Meso-NHM-based model forecast charts available on the Internet

Levels	Content	Initial Time	Forecast Hours	Area
Surface	Simulated IR imageries overlaid with rain areas	00, 06, 12 and 18 UTC	06, 12, 18, …72	8 – 46.5 °N, 85 – 148 °E
	Air temperature		00, 06, 12, …72	
	Mean sea level pressure			
	Wind			

	Relative humidity and streamline			
850 hPa	Wind			
	Relative vorticity and streamline			
700 hPa	Wind			
	Relative humidity and streamline			
500 hPa	Wind			
	Geopotential height			
200 hPa	Wind			
	Jet stream and streamline			

4.3.3.4 Products from global models

Forecast products based on the global models from ECMWF, JMA, NCEP, UKMO, CMA and KMA were presented to the forecasters in higher temporal resolution (down to 3-hourly intervals generally and down to 1-hourly intervals for zoom-in surface charts for NCEP) over the first 3- to 5-day of the forecast range.

4.3.4 Operational techniques for application of NWP products

4.3.4.1 In operation

4.3.4.1.1 AIR/NHM

Post-processed maximum and minimum temperatures from Meso-NHM based on Kalman filtering and linear regression for various locations in Hong Kong were routinely generated for reference of the forecasters.

A vortex tracker specially designed to work on the high resolution model outputs of Meso-NHM is in operation. Taking the mean sea level pressure field and circulation at 850 hPa as inputs, the vortex tracker can effectively distinguish between lee lows and tropical cyclones from the high resolution model outputs of Meso-NHM.

A tropical cyclone forecasting tool called Meso-NHM TC Nowcast was in operation. By extrapolating the movement of the tropical cyclone vortex extracted from Meso-NHM along the warning track, forecast time series of wind strength and pressure at various locations in Hong Kong are produced to facilitate forecasters' assessment of the risk of occurrence of strong and gale force winds over the territory in the next 24 hours.

A TC structure forecasting tool based on the outputs from Meso-NHM was developed. It provides the predicted evolution of various TC wind radii, presented in both textual and graphical formats for the ease of user digestion.

Time-lagged ensemble QPF products were developed using rainfall forecasts from successive runs of Meso-NHM and RAPIDS-NHM. In each NHM domain, direct model output of QPF at a given forecast time from all available model runs were combined to generate gridded time-lagged ensemble rainfall. Forecast rainfall maps of the ensemble mean and 75th-percentile were generated where the latter showed an improved skill over individual runs when verified against gridded quantitative precipitation estimates (QPE) using satellite or radar data.

4.3.4.1.2 AVM

In support of short-term aviation weather forecasts for HKIA, a novel suite of aviation-specific products were developed taking advantage of the very high spatial resolution of the inner AVM-HKA domain. These include (i) forecast potential of significant low-level windshear for each arrival and departure runway corridor; and (ii) forecast spatial distribution of low-level turbulence intensity around HKIA as represented by the eddy dissipation rate (EDR).

Algorithms were developed for simulation of cloudy radiances using 600-m resolution AVM-PRD output based on RTTOV, a fast radiative transfer algorithm. The resulting simulated satellite cloud images were generated at high frequency of every 10 minutes and provided useful guidance for diagnosing timing of weather features as well as evaluating model performance in real-time.

4.3.4.1.3 Significant Convection Forecast Products in support of Air Traffic Management

Using QPF output from NWP model as basis together with modifications by aviation weather forecasters, significant convection forecasts up to 12 hours over key air traffic control areas of the Hong Kong Flight Information Region (HKFIR) are provided at 3-hourly intervals in support of air traffic management (ATM) (Cheung and Lam 2011a).

Blending radar-based extrapolation nowcast with phase-adjusted model QPF from RAPIDS-NHM was implemented for the airspace within 128km from Hong Kong. Blended forecasts were used to generate 6-hour forecasts of significant convection over selected critical Air Traffic Control (ATC) regions including 20 nautical miles of HKIA and the closest holding areas for arrival flights. It was updated every 12 minutes to cope with changeable weather situations. This product was merged with the 12-hour significant convection forecast to support airport operations, as well as the airport and airspace capacity forecasts by local ATC.

In 2016, the QPF output from ECMWF EPS consisting of 50 members at 0.25-degree resolution replaced the QPF output from ECMWF deterministic model as the first guess for the 12-hour forecast.

4.3.4.1.4 Others

Utilizing global and regional NWP model outputs, a post-processing algorithm is used to produce site-specific objective consensus total cloud cover forecast. The algorithm employs downscaling and model output statistics weighting techniques. The cloud cover forecast is ingested into an empirical sea breeze forecast model used at the Hong Kong International

Airport and it improves the accuracy of sea breeze forecast with higher detection rate and lower false alarm ratio.

Probability forecasts of wind speed and crosswind at HKIA exceeding pre-defined thresholds for up to 36 hours ahead during TC situations, generated using the ECMWF EPS (Cheung and Lam 2011b), continued under trial operation to support aviation users in risk assessment for flight planning. To facilitate user interpretation of uncertainty information, the wind forecasts were accompanied by probabilistic forecasts of tropical cyclone distance from HKIA.

4.3.4.2 Research performed in this field

When extending OCF to a hill-top location in Hong Kong, substantial cold bias was found in the daily maximum temperature under fine weather situation. A study was underway to explore different multi-variate model post-processing methods to improve the hill-top forecasts.

Another research project on 3-dimensional wind downscaling was initiated with a view to incorporating the orographic effect on both wind speed and wind direction by running a mass-consistent model. Initial results from case study indicated that realistic looking wind fields can be produced with improvement over the direct model output.

In connection with the domain extension of AVM-xHKA, research was performed in improving the formulation of boundary layer turbulence process. Preliminary results indicated improved temperature and wind response, particularly during windshear-conducive weather regimes with rapidly fluctuating flows as observed by LIDARs.

4.3.5 Ensemble Prediction System

An in-house 20-member mesoscale ensemble prediction system (MEPS) based on dynamical downscaling of NCEP GEFS output using the WRF model at a horizontal resolution of 10 km continued to provide real-time probabilistic forecast guidance up to 3 days ahead (Hon, 2015). A suite of probabilistic forecast products were developed and made available for forecasters' reference including exceedance probabilities of rainfall, wind speed and temperature, as well as tropical cyclone strike probability. The MEPS provided useful indication of severe weather along the South China coastal areas, particularly for tropical cyclones and rainstorm cases (Hon and Hon, 2016).

Algorithm was developed for the simulation of cloudy radiances using MEPS output based on RTTOV, a fast radiative transfer model. The resulting 20-member simulated satellite cloud image stamp map products were made available in real time in support of significant convection forecasts (Song, Lee and Hon, 2017).

Experiments were also conducted on the feasibility of convective-scale ensemble prediction and indicated some potential benefits in certain severe convection cases (Tsoi and Hon, 2016). Additionally, the use of ensemble-based data assimilation techniques (such as the Ensemble Kalman Filter) would be explored for ingestion of new remote-sensing observations such as large-area radar composites and Himawari-8 cloudy radiances.

4.4 Nowcasting and Very Short-range Forecasting Systems (0-12 hrs)

4.4.1 Nowcasting system

4.4.1.1 In operation

4.4.1.1.1 SWIRLS

SWIRLS (Short-range Warning of Intense Rainstorms in Localized Systems) (Li & Lai 2004) is a radar-based multi-functional nowcasting system with applications in the warning of rainstorms, floods, landslips, thunderstorms, hail and gust. It employs variational optical flow and semi-Lagrangian advection to predict the motion of rainy areas and severe weathers (Woo & Wong, 2017).

Major products of SWIRLS include:

(i) Quantitative Precipitation Estimates (QPE), based on radar, rain gauges and a blending of both by co-Kriging analyses (Yeung *et al*. 2010; Yeung *et al*. 2011).
(ii) Quantitative Precipitation Forecast (QPF) by extrapolation of radar echoes up to 6 hours over a domain of about 240 km x 240 km centred at Hong Kong;
(iii) Forecast of thunderstorm, hail and gust based on radar signatures and model analyses;
(iv) Automatic Rainstorm Related Objective Warnings (ARROW) to provide local warning guidance on rainstorms, floods, landslips, thunderstorms, hail and gust;
(v) SWIRLS Integrated Panel (SIP) to feature a consolidated view of essential tools supporting rainstorm nowcast and warning;
(vi) Special Tips on Intense Rainfall (STIR) to automatically generate human comprehensible messages based on data;
(vii) Probabilistic Quantitative Precipitation Nowcast (PQPN) based on "SWIRLS Ensemble Rainfall Nowcast (SERN)", an ensemble comprising 36 members;
(viii) SWIRLS Time-series And Mapped Probabilities (STAMP) to visualize PQPN and related products for operation and research;
(ix) Location-specific rainfall nowcast for the public through Internet website and mobile apps with notifications;
(x) SWIRLS Interactive TephiViewer which computes atmospheric instability and the possibility of orographic rainfall;
(xi) "TC Module" that enhances performance in tropical cyclone (Woo et al. 2014); and
(xii) Verification of system performance, including ARROW and weather warnings, by traditional and progressive verification scheme.

In 2016, SWIRLS was enhanced as follows:

(i) Development of location-specific lightning nowcast with verification. Services for the public and special users will commence in 2017; and
(ii) Update to radar-rainfall (Z-R) parameters to enhance the accuracy of QPE and QPF.

4.4.1.1.2 ATNS

The Aviation Thunderstorm Nowcasting System (ATNS) (Li 2009) is used to provide thunderstorm nowcasting products for HKIA and HKFIR. Tracking algorithm is based on TREC, and semi-Lagrangian advection scheme is used to generate the forecast radar reflectivity field. Time series on the severity of the forecast reflectivity in 6-minute interval at strategic locations (air traffic control "way-points") up to the next hour are also generated. Users from ATM and airlines could make reference to the storm severity at various way-

points from a web-based display integrating GIS information, forecast reflectivity distribution and the aforementioned time series products. "Amber" and "Red" alerts that correspond to radar reflectivity exceeding 33 dBZ and 41 dBZ respectively affecting the way-points are also provided on the web display. Further development work were underway to enhance its capabilities and performance including providing route and trajectory based nowcasting products as well as fine-tuning the alerting thresholds to warn more effectively air traffic manager regarding the impacts to air traffic over HKFIR.

4.4.1.1.3 Airport Thunderstorm and Lightning Alerting System (ATLAS)

ATLAS provides cloud-to-ground (C-G) lightning alerts over HKIA for the protection of the personnel working on apron based on actual lightning strikes recorded by the lightning detection systems, as well as forecast lightning by storm tracking algorithm (TREC) and time-lag-ensemble storm tracking method (Li and Lau, 2008). When cloud-to-ground lightning was detected within 16km from the airport, ground operators will be alerted to switch to Bluetooth headsets - Wireless Headset Procedure. "Amber" alert will be issued if cloud-to-ground lightning with intense radar echo is detected within 10km or predicted within 5 km from the centre of the airport. Separate "Red" alerts will be issued for zone A (comprising the passenger and cargo terminal) and zone B (the rest of the airport island) when C-G lightning occurs or is predicted to occur within 1 km of the zones.

4.4.1.1.4 Lightning Nowcasting System (LiNS)

LiNS provides C-G lightning strokes forecast to specialized users or corporate clients for assessing the needs for early preventive actions due to lightning threats. Forecasts of regional lightning strokes up to 2 hours ahead are generated using TREC and its ensemble motion vectors, semi-Lagrangian advection scheme and the temporal trend of the lightning intensity. Both graphical products and text alerts are distributed to the users in every 6 minutes interval. Optimization on defining thresholds for the LiNS alert levels due to increased resilience of the power lines has been completed and new, higher thresholds have been put to operation.

4.4.1.2 Research performed in this field

4.4.1.2.1 SWIRLS

Development of the community version of SWIRLS (Com-SWIRLS) continued with a severe weather module in the pipeline. Collaboration with interested NMHSs deepened with more technical support provided, some of which under Aviation Research Demonstration Project (AvRDP).

The research project to develop an algorithm that predicts the evolution of radar echoes using deep-learning recurrent neural network (Shi *et al.*, 2015) brought two enhanced algorithms (Shi *et al.*, 2017). Verification showed superior performance in 2-hour nowcast for rainfall intensity ranging from 0.5 to 30 mm/h.

Algorithms to derive cloud mask, cloud types and cloud top height using Himawari-8 data, partially based on EUMETSAT NWC SAF codes, were developed. Experimental products on "Convective Initiation" (CI) and "Rapid Development Thunderstorms (RDT)" were implemented and under fine-tuning.

4.4.1.2.2 ATNS

Parallel testing to evaluate the performance of different echo tracking algorithms, namely, TREC and ROVER was conducted. Verification results showed that ROVER performed better than TREC. Further investigation on the ROVER motion field under TC situation was undergoing to determine if the new tracking algorithm could replace the operational one. On the other hand, a 3D tracking and extrapolation algorithm which is capable to produce a volumetric nowcasting output was being developed and under testing.

4.4.1.2.3 ATLAS

A new set of lightning detection processor was under trial in 2016. Use of new lightning data for ATLAS and impact to lightning alerts from the user's perspective has been conducted. Full operation and adaptation of the new lightning dataset was expected in 2017.

4.4.1.2.4 LiNS

The use of LiNS to provide lightning alerting service for a cable car company was undergoing. Feasibility of using the system output for public lightning service has been confirmed. New service of lighting alert for the general public was under development and testing.

4.4.2 Models for Very Short-range Forecasting Systems

4.4.2.1 In operation

4.4.2.1.1 Rainstorm Analysis and Prediction Integrated Data-processing System (RAPIDS)

RAPIDS provides QPF for the next 6 hours at 2 km resolution (Wong and Lai 2006, Wong *et al*. 2009). The system blends the outputs from SWIRLS and RAPIDS-NHM at 6-minute intervals with respective weightings determined from real-time verification of their precipitation predictions. Phase correction to correct spatial errors in the forecast precipitation field in RAPIDS-NHM was included. To correct the biases in rainfall intensity occasionally found in RAPIDS-NHM forecast, an intensity correction scheme, which is based on comparing cumulative distribution of rainfall intensity from SWIRLS rainfall analysis and RAPIDS-NHM short-term forecast, was also implemented. Using the time-lagged ensemble approach, probability forecasts of precipitation out to 6 hours are also generated by the system.

4.4.2.1.2 Six-hourly Short-term QPF System

The short-term QPF system facilitates forecaster's preparation of a 6-hourly rainfall forecast over Hong Kong out to 30 hours. Inputs included the QPF from SWIRLS, RAPIDS, RAPIDS-NHM, Meso-NHM, global models of JMA, ECMWF, NCEP, UKMO and ECMWF EPS. QPF from global models and Meso-NHM in heavy rain are calibrated with adaptive parameters for improved performance. A "blended" QPF derived as the average of constituent objective guidance was also provided.

4.4.2.2 Research performed in this field

4.4.2.2.1 Significant convection forecast

Testing of a trend-based blending of ATNS and RAPIDS-NHM simulated reflectivity produced promising results (Cheung, et al. 2014). The algorithm will be put to routine running to collect more cases to demonstrate its performance.

4.4.2.2.2 Satellite based nowcasting technique development

Satellite Himawari-8 based split-window and machine learning techniques for identification of significant convection, turbulence and icing have been developed and under testing. Nowcasting system based on tracking and extrapolation for satellite based significant convection has been developed and under testing. For turbulence and icing, use of NWP simulated satellite imagery for producing a short term forecast will be tested.

4.5 Specialized numerical predictions

4.5.1 Assimilation of specific data, analysis and initialization

4.5.1.1 In operation

4.5.1.1.1 SLOSH (Storm Surge Model)

The forecast position, minimum pressure and storm size of tropical cyclones at 6-hourly intervals from 48 hours before the time of closest approach to Hong Kong to 24 hours after are used as input to the SLOSH.

4.5.1.1.2WAVEWATCH III (Wave Model)

Forecast surface wind data from JMA based on 00 and 12 UTC are used as input for the areas:
(1) 5 – 35 °N, 105 – 135 °E with grid resolution 1.25° × 1.25°,
(2) 21.25 – 22.5 °N, 113.75 – 115 °E with grid resolution 0.25° × 0.25°.

4.5.1.1.3 Accident Consequence Assessment System

The Accident Consequence Assessment System is used to assess the consequence of nuclear accident occurring at nearby nuclear power plants and to simulate the dispersion of radioactive materials from nuclear accident around the world. It consists of two systems, namely the RODOS (Real-time Online DecisiOn Support) system and FLEXPART (FLEXible PARTicle dispersion model).

The RODOS system, which was developed under the European Commission's Framework Programmes, has been adopted by HKO to assess the consequence of nuclear accident occurring at nuclear power plants at Daya Bay and other places in Guangdong, China. The current version of RODOS installed at HKO is the Java-based RODOS (JRODOS July 2014 Update 3 Version).

The RODOS system was configured and initialised with fixed background data including land use, nuclear reactor sites information, dose intervention levels for countermeasures, and source term library. The following data is assimilated during a model run:

(a) Source term of the radioactive release including quantity of different nuclides and their release durations.

(b) Meteorological data ingested from prognostic NWP data or via manual input. Prognostic model data at multiple levels for the area 18 – 28 °N, 108 – 118 °E from Meso-NHM based on 00 and 12 UTC runs are available regularly as input. Alternatively, the user can manually input the meteorological data including wind speed and direction, atmospheric stability condition and precipitation rate.

The FLEXPART (FLEXible PARTicle dispersion model), a Lagrangian transport and dispersion model for the simulation of long range atmospheric transport process of radioactive materials, was installed in HKO in 2016. The version of FLEXPART installed is 9.02. The following prognostic model data at multiple levels are retrieved regularly as input for driving the FLEXPART simulations:

(a) ECMWF 0.5-degree resolution data with global coverage,

(b) ECMWF 0.125-degree resolution data covering eastern Asia (18-30°N, 108-125°E), and

(c) NCEP GFS 1-degree resolution data with global coverage.

4.5.2 Specific models

4.5.2.1 In operation

4.5.2.1.1 Model for Rio 2016 Olympics

A WRF model simulation system was configured and run for Rio, Brazil, in support of the windsurfing team of Hong Kong to participate in the Rio 2016 Olympics. Forecast verification was carried out on the TAF issued by the airports near the sports venue, and the results were presented to the team along with other potential forecast products including high-resolution model simulation and a forecasting tool on sea-breeze onset.

4.5.2.1.2 SLOSH (Storm Surge Model)

A general description of SLOSH is summarised as follows:

Governing equation	Transport equations of motion
Prognostic variables	Horizontal components of transport, water height
Spatial grid and resolution	A curvilinear polar grid, from 1 km resolution near the centre of the Hong Kong Basin to 7 km in open sea, 83 × 146 grid points
Terrain and bathymetry	Land topography and water depth at sea points
Initialization	Initialization time proposed by Jelesnianski *et al.* (1992). Static height elevations due to storm's pressure drop at the initial time are added to the initial quiescent water level.

Boundary conditions	Scheme proposed by Jelesnianski *et al.* (1992) to cater for different water depths
Driving forces	Simplified model storm (Jelesnianski and Taylor, 1973)
Numerical technique	Explicit finite difference scheme

Further details can be found in Jelesnianski *et al.* (1992).

4.5.2.1.3 WAVEWATCH III (Wave Model)

A general description of WAVEWATCH III is summarised as follows. Nested model runs are implemented for the areas:
(1) 5 – 35 °N, 105 – 135 °E with grid resolution 1.25° × 1.25°,
(2) 21.25 – 22.5 °N, 113.75 – 115 °E with grid resolution 0.25° × 0.25°.

Governing equation	Spectral action density balance equation
Prognostic variables	Wave action density spectrum
Spatial grid and resolution	Mercator projection for the areas: (1) 5 – 35 °N, 105 – 135 °E, 1.25° × 1.25° resolution, 27 × 27 grid points including boundary data zone (2) 21.25 – 22.5 °N, 113.75 – 115 °E, 0.25° × 0.25° resolution, 8 × 8 grid points including boundary data zone
Bathymetry	Water depth at sea points (SRTM)
Intra-spectral grid	24 directions with 15° increment, 25 logarithmic frequency grid points
Initial conditions	Parametric fetch-limited JONSWAP spectrum
Boundary conditions	(1) For the large area run, initial conditions applied as constant boundary conditions (2) For the small area run, model outputs from the large area run are used as input boundary conditions
Source term (input and dissipation)	Tolman and Chalikov parameterization
Source term (nonlinear interactions)	Discrete interaction approximation
Source term (bottom friction)	JONSWAP parameterization
Propagation scheme	Ultimate Quickest scheme with averaging
Numerical technique	Fractional step method

Further details can be found in Tolman (2002).

4.5.2.1.4 Accident Consequence Assessment System

General descriptions of RODOS and FLEXPART are summarised as follows.

(a) RODOS

RODOS employs an atmospheric dispersion and deposition model called ATSTEP (Päsler-Sauer, J, 2007), which is a short range Gaussian puff model developed especially for quick simulations of accidental releases of airborne radioactive materials.

In ATSTEP, time-integrated elongated puffs are released. The transport of each elongated puff is achieved by two trajectories attached to both ends of the puff. These pairs of trajectories follow the inhomogeneous and variable 2-dimensional wind fields step by step. The elongated puffs perform all the necessary changes in position, shape, and orientation, such as stretching, rotations, shrinking, and sideways drift.

Because of the large size of the elongated puffs, the plume can be represented by a relatively small number of puffs. Correspondingly, the number of time steps needed for the simulation of the release and the transport is small. The elongated puff approximation reduces the computing time of the model. Less than 10 minutes is required for a complete dispersion and contamination prognosis with releases over several hours.

In ATSTEP, the following phenomena are considered in the modelling of atmospheric dispersion and the radiological situation: time dependent meteorology data, time dependent nuclide-group specific release rates, thermal energy and rise of the puffs released, dry and wet deposition and corresponding depletion of the cloud, gamma radiation from cloud and from ground, radioactive decay and build-up of daughter nuclides, and potential doses.

Regarding the spatial resolution of the results, for a range of 100 km from the release location, the innermost region has 20 × 20 grid cells with resolution of 0.25 × 0.25 km^2. Four more square frames containing cells with edge of double size, 4-fold, 8-fold and 16-fold size, surround this region. In the outermost cell, there are 50 × 50 grid cells each of 4 × 4 km^2.

(b) FLEXPART

FLEXPART is a Lagrangian particle dispersion model that simulates the long-range transport, diffusion, dry and wet deposition and radioactive decay of materials released from point, line, area or volume sources.

In FLEXPART, turbulent motions for wind components are parameterized assuming a Markov process based on the Langevin equation. Parameterized random velocities in the atmospheric boundary layer are calculated by surface sensible heat fluxes, surface stresses and other meteorological data. Due to the absence of suitable turbulence parameterizations above the atmospheric boundary layer, a constant vertical diffusivity 0.1 m^2/s is used in the stratosphere, whereas a horizontal diffusivity 50 m^2/s is used in the troposphere.

Radioactive decay is accounted for by reducing the particle mass according to the exponential decay equation with given half-life. Wet deposition also takes the form of an exponential decay process by using scavenging coefficients. Dry deposition is described by a deposition velocity. The deposition velocity of a gas is calculated with the resistance

method. FLEXPART also includes a moist convective parameterization scheme to represent convective transport in a particle dispersion model.

Further details of FLEXPART can be found in Stohl et al. (2005).

4.5.2.2 Research performed in this field

A system to post-process JRODOS output data and display tailor-made products automatically was developed and put into operation in 2016.

Studies to compare the simulation results of the long range dispersion models FLEXPART and HYSPLIT were carried out. Preliminary analysis showed that the forecast trajectories by both models were similar, but there were some differences in the air concentration and deposition fields (Chan, et al., 2016).

4.6 Extended range forecasts (ERF) (10 days to 30 days)

4.6.1 Models

4.6.1.1 Research performed in this field

A collaborative research project with a local power company was underway on the automatic daily max/min temperature forecasts for Day 10-14 based on EPS data with impact on power consumption management as the main thrust. The post-processing of the probability distribution function were also being considered.

4.7 Long range forecasts (LRF) (30 days up to two years)

4.7.1 In operation

HKO operates a suite of global-regional spectral climate models (2-tier) adapted from the Experimental Climate Prediction Center, USA. The model suite generates seasonal temperature and rainfall forecasts for Hong Kong, China. Products are made available to the general public via HKO's Internet website.

4.7.2 Research performed in this field

Various post-processing methods were developed to calibrate direct model output from major climate prediction centres to produce categorical and quantitative forecasts of monthly/seasonal temperature and rainfall. These calibrated forecasts generally perform better than the direct model output.

4.7.3 Operationally available products

Graphical representation of seasonal temperature and rainfall anomaly forecasts over southern China are available on HKO's website.

5 Verification of prognostic products

5.1 Annual verification summary

Verifications of forecasts generated by Meso-NHM are conducted on a routine basis. Forecast parameters including zonal and meridional winds, temperature, pressure/geopotential heights and relative humidity at a number of model levels are verified against respective model analyses and rawinsonde observations for the area 10 – 40 °N, 95 – 135 °E. The monthly verification results of Meso-NHM 12 UTC runs for 2016 are presented in Appendix I. Verification of SLOSH outputs during the passage of a tropical depression in May, tropical cyclones Nida, Dianmu, Sarika and Haima from August to October 2016 is shown in Appendix II. Verification of prognostic products generated by WAVEWATCH III is shown in Appendix III.

6 Plans for the future (next 4 years)

6.1 Development of the GDPFS

6.1.1 The next-generation TIPS system will be developed on a GIS-enabled platform to facilitate efficient ingestion of various TC-related observations and information.

6.2 Planned Research Activities in NWP, Nowcasting, Long-range Forecasting and Specialized Numerical Predictions

6.2.1 Planned Research Activities in NWP

(i) Research on nowcasting lightning based on radiometer retrieved profiles would be undertaken.

(ii) It is planned to develop a sophisticated and integrated operational marine forecasting system to support the Central Forecasting Office's operation on provision of marine meteorological services.

(iii) Development and fine-tuning of physical parameterisation suitable for meso- and micro-scale models in relation to boundary layer and cumulus convection processes.

(iv) Assimilation of remote-sensing observations including satellite radiance and radar reflectivity through conventional and ensemble-based methods would continue.

(v) Extension of OCF to global cities.

(vi) Continue research study on 3-dimensional wind downscaling by mass-consistent model.

(vii) Integration of storm tide, through extracting tidal constituents from a global tide model - a new feature in the new version of the SLOSH storm surge model acquired from NOAA, in addition to storm surge for each grid of the SLOSH basin into the Operational Storm Surge Prediction System for trial operation.

(viii) Development of an integrated operational marine forecasting system to support the provision of marine meteorological services. In this connection, a new version of WaveWatch III model would be adopted to generate the wave and swell products.

6.2.2 Planned Research Activities in Nowcasting

(i) Further testing under AvRDP the enhanced blending of NWP-derived radar product and nowcasting output for aviation application for the generation of seamless forecast from 1-12 hours.

(ii) Continue research on the use of NWP simulated satellite imagery for producing a short term forecast of icing and turbulence.

(iii) Development of a new version of Com-SWIRLS, which will be installation-free and cloud-ready, incorporating standard programming interface and featuring user-friendly web-based interface in manual / demonstration mode.

(iv) Enhancement of the operational SWIRLS with increased spatial resolution, more ensemble members, and incorporation of advanced nowcasting techniques.

6.2.3 Planned Research Activities in Long-range Forecasting

Efforts to utilise digital data provided by WMO GPCs and to investigate various statistical downscaling and post-processing techniques to improve the skill of monthly/seasonal temperature and rainfall forecasts of Hong Kong would continue.

7 References

Arakawa, A. and W.H. Schubert, 1974: Interaction of a cumulus cloud ensemble with the large-scale environment, Part I. *J. Atmos. Sci.*, **31**: 674-701.

Beljaars, A., 1995: The parametrization of surface fluxes in large-scale models under free convection. *Quart. J. Roy. Meteor. Soc.*, **121**, 255-270.

Beljaars, A. C. M. and A. A. M. Holtslag, 1991: Flux parameterization and land surfaces in atmospheric models. *J. Appl. Meteor.*, **30**, 327-341.

Chan, P.K.Y, W.H. Leung and W.M. Ma, 2016: A Comparative Study of Atmospheric Dispersion Models. *30th Guangdong-Hong Kong-Macao Technical Seminar on Meteorological Technology,* 20 – 22 April 2016.

Chan, P.W. and K.K. Hon, 2015: Performance of super high resolution numerical weather prediction model in forecasting terrain-disrupted airflow at the Hong Kong International Airport: case studies. *Meteorol. Appl.*, **23**, 101-114.

Chan, P.W. and K.K. Hon, 2016: Observation and numerical simulation of terrain-Induced windshear at the Hong Kong International Airport in a planetary boundary layer without temperature inversions. Advances in Meteorology, vol. 2016, Article ID 1454513, 9 pages, 2016.

Chan, P.W., N.G. Wu, C.Z. Zhang, K.K. Hon and W.J. Deng, 2017: The first complete dropsonde observation of a tropical cyclone by the Hong Kong Observatory at the South China Sea. *Weather*, manuscript accepted. DOI: 10.1002/wea.3095

Cheung, P. and C.C. Lam, 2011a: Development of significant convection forecast product and service for air traffic flow management in Hong Kong. *Second Aviation, Range and Aerospace Meteorology Special Symposium on Weather-Air Traffic Management Integration*, Seattle, WA, 23-27 January 2011.

Cheung, P. and C.C. Lam, 2011b: Objective calibrated wind speed and crosswind probabilistic forecasts for the Hong Kong International Airport. *Second Aviation, Range and Aerospace Meteorology Special Symposium on Weather-Air Traffic Management Integration*, Seattle, WA, 23-27 January 2011.

Cheung, P., P.W. Li and W.K. Wong, 2014: Blending of Extrapolated Radar Reflectivity with Simulated Reflectivity from NWP for a Seamless Significant Convection Forecast up to 6 Hours. *17th Conference on Aviation, Range, and Aerospace Meteorology*, Phoenix, Arizona, USA, 4-8 January 2015.

Donelan, M.A., B.K. Haus, N. Reul, W.J. Plant, M. Stiassnie, H.C. Graber, O.B. Brown and E.S. Saltzman, 2004: On the limiting aerodynamic roughness of the ocean in very strong winds. *Geophys. Res. Let.*, **31**, L18306.

Engel, C. and E. Ebert, 2007: Performance of hourly operational consensus forecasts (OCF) in the Australian region. *Wea. Forecasting*, **20**, 101-111.

Fairall, C.W., E.F. Bradley, J.E. Hare, A.A. Grachev and J.B. Edson, 2003: Bulk parameterization of air-sea fluxes: Updates and verification for the COARE algorithm. *J. Climate*, **16**, 571-591.

Hon, K.K., 2015: First studies on mesoscale ensemble prediction over the South China coastal areas. *29th Guangdong-Hong Kong-Macao Technical Seminar on Meteorological Technology,* 20 – 22 January 2015, Macau.

Hon, K.K. and P.W. Chan, 2014: Sub-kilometer simulation of terrain-disrupted airflow at the Hong Kong International Airport – Aviation applications and inter-comparison with LIDAR observations. Conference on Mountain Meteorology 2014, San Diego, CA, 22 – 25 August 2014.

Hon, K.K. and P.W. Chan, 2015: Sub-kilometre simulation of terrain-disrupted airflow associated with aircraft diversion at the Hong Kong International Airport. *33rd International Conference on Alpine Meteorology*, Innsbruck, Austria, 31 August – 4 September 2015.

Hon, W.Y. and K.K. Hon, 2016: First studies on mesoscale ensemble prediction of tropical cyclones over the South China coastal areas, 30th Guangdong-Hong Kong-Macau Seminar on Meteorological Technology, 20-22 April 2016, Guangzhou.

Jelesnianski, C.P., J. Chen and W.A. Shaffer, 1992: SLOSH Sea, Lake and Overland Surges from Hurricanes. *NOAA/NWS Technical Report NWS 48*.

Jelesnianski, C.P. and A.D. Taylor, 1973: A preliminary view of storm surges before and after storm modifications. *NOAA Technical Memorandum ERL WMPO-3*.

Kitagawa, H., 2000: Radiation process. *Report of Numerical Prediction Division*, **46**, 16-31 (in Japanese).

Li, P.W. and E.S.T. Lai, 2004 : Short-range Quantitative Precipitation Forecasting in Hong Kong, *J. Hydrol*. **288**, 189-209.

Li, P.W. and D.S. Lau, 2008 : Development of a Lightning Nowcasting System for Hong Kong International Airport. *Presented in the 13th Conference on Aviation, Range and Aerospace Meteorology*, 20-24 January 2008, New Orleans, Louisiana, USA.

Li, P.W., 2009: Development of a thunderstorm nowcasting system for Hong Kong International Airport, AMS Aviation, Range, *Aerospace Meteorology Special Symposium on Weather-Air Traffic Management Integration*, Phoenix, Arizona, 11-15 Jan 2009.

Nakanishi, M. and H. Niino, 2004: Improvement of the Mellor-Yamada level 3 model with condensation physics: Its design and verification. *Boundary-Layer Meteorol.*, **112**, 1-31.

Päsler-Sauer, J., 2007: Description of the Atmospheric Dispersion Model ATSTEP – Version RODOS PV 6.0 Final, RODOS(RA2)-TN(04)-03, Forschungszentrum Karlsruhe GmbH, Karlsruhe.

Saito, K., T. Fujita, Y. Yamada, J. Ishida, Y. Kumagai, K. Aranami, S. Ohmori, R. Nagasawa, S. Kumagai, C. Muroi, T. Kato, H. Eito and Y. Yamazaki, 2006: The operational JMA nonhydrostatic model. *Mon. Wea. Rev*., **134**, 1266-1298.

Shi, X.J., Z.R. Chen, H. Wang, D.Y. Yeung, W.K. Wong and W.C. Woo, 2015: Convolutional LSTM Network: A Machine Learning Approach for Precipitation Nowcasting, Advances in Neural Information Processing Systems **28**, arXiv:1506.04214 **[cs.CV]**

Shi, X.J., Z.H. Gao, L. Lausen, H. Wang, D.Y. Yeung, W.C. Woo, 2017: Deep Learning for Precipitation Nowcasting: A Benchmark and A New Model, Advances in Neural Information Processing Systems **30**, arXiv:1706.03458 **[cs.CV]**

Skamarock, W. C. and J. B. Klemp, 2008: A Time-Split Nonhydrostatic Atmospheric Model for Weather and Forecasting Applications. J. Comp. Phys., 227, 3465-3485.

Song, M.K., L.S. Lee and K.K. Hon, 2017: Development of public weather services of the Hong Kong Observatory. Advances in Meteorological Science and Technology, **1**, 227-237.

Stohl, A., C. Forster, A. Frank, P. Seibert, and G. Wotawa, 2005: Technical Note : The Lagrangian particle dispersion model FLEXPART version 6.2. *Atmospheric Chemistry and Physics*, **5**, 2461-2474.

Tiedtke M., 1989: A comprehensive mass flux scheme for cumulus parameterization in large-scale models. *Mon. Wea. Rev.*, **117**, 1779-1800.

Tolman H.L., 2002: User manual and system documentation of WAVEWATCH-III version 2.22. *NOAA/NWS/NCEP/MMAB Technical Note 222*.

Troen I. and L. Mahrt, 1986: A simple model of the atmospheric boundary layer: Sensitivity to surface evaporation. *Boundary Layer Meteorl.*, **37**, 129-148.

Tsoi, T.S. and K.K. Hon, 2016: Experiments on cloud-resolving ensemble prediction of severe convection over the coast of Guangdong, 30th Guangdong-Hong Kong-Macau Seminar on Meteorological Technology, 20-22 April 2016, Guangzhou.

Woo, W.C., K.K. Li, Michael Bala, 2014: An Algorithm to Enhance Nowcast of Rainfall Brought by Tropical Cyclones Through Separation of Motions. *Tropical Cyclone Research and Review*, 3(2), 111-121.

Wong, W.K., 2011: Development of Operational Rapid Update Non-hydrostatic NWP and Data Assimilation Systems in the Hong Kong Observatory, *Technical Reports of the Meteorological Research Institute No. 65: "International Research for Prevention and Mitigation of Meteorological Disasters in Southeast Asia"*, p.87-100.

Wong, W.K. and E.S.T. Lai, 2006: RAPIDS – Operational Blending of Nowcast and NWP QPF. *presented in the 2nd International Symposium on Quantitative Precipitation Forecasting and Hydrology*, 4-8 June 2006, Boulder, Colorado, USA.

Wong, W.K., C.S. Lau and P.W. Chan, 2013: Aviation Model: a fine-scale numerical weather prediction system for aviation applications at the Hong Kong International Airport. *Advances in Meteorology*, Vol. 2013, Article ID 532475, 11 pages.

Wong W.K., M.K. Or, P.W. Chan and C.M. Cheng, 2011: Impact of Radar Retrieval Winds on Data Assimilation and Forecast of a Mesoscale Convective Storm using Non-Hydrostatic Model. *14th Conference on Mesoscale Process*, American Meteorological Society, Los Angeles, USA, 1-4 August 2011

Wong, W.K., S. Sumdin, and S.T. Lai, 2011: Development of Air-Sea Bulk Transfer Coefficients and Roughness Length in JMA Non-Hydrostatic Model, *Technical Reports of the Meteorological Research Institute No. 65: "International Research for Prevention and Mitigation of Meteorological Disasters in Southeast Asia"*, p.82-85.

Wong, W.K., S.M. Tse and P.W. Chan, 2013: Impacts of Reconnaissance Flight Data on Numerical Simulation of Tropical Cyclones over South China Sea, *Met. Application* DOI: 10.1002/met.1412.

Wong, W.K., L.H.Y. Yeung, Y.C. Wang and M. Chen, 2009: Towards the Blending of NWP with Nowcast — Operation Experience in B08FDP, *WMO Symposium on Nowcasting*, 30 Aug-4 Sep 2009, Whistler, B.C., Canada.

WOO, WC., W.K. Wong: Operational Application of Optical Flow Techniques to Radar-Based Rainfall Nowcasting, *Atmosphere* **2017**, *8*(3), 48; doi: 10.3390/atmos8030048

Yabu, S., S. Murai and H. Kitagawa, 2005: Clear sky radiation scheme. *Report of Numerical Prediction Division*, **51**, 53-64 (in Japanese).

Yeung, H.Y., C. Man, S.T. Chan and A. Seed, 2011: Application of radar-raingauge co-kriging to improve QPE and quality control of real-time rainfall data. *International Symposium on Weather Radar and Hydrology*, 18-21 April 2011, Exeter, U.K.

Appendix I — Summary of Verification of Prognostic Products Generated by Meso-NHM 12 UTC Runs for 2016 (Verification Area: 10 – 40 °N, 95 – 135 °E)

Table 1a. RMS error of mean sea level pressure against analysis (in hPa)

Hours	Jan	Feb	Mar	Apr	May	Jun	Jul	Aug	Sep	Oct	Nov	Dec	Average
24	1.5	1.7	1.4	1.3	1.4	1.3	1.3	1.3	1.3	1.4	1.5	1.5	1.4
72	3.2	2.9	2.6	2.0	2.1	2.0	1.9	2.4	2.3	2.4	2.4	2.7	2.4

Table 1b. RMS error of mean sea level pressure against observations (in hPa)

Hours	Jan	Feb	Mar	Apr	May	Jun	Jul	Aug	Sep	Oct	Nov	Dec	Average
24	1.5	1.7	1.3	1.3	1.4	1.2	1.3	1.1	1.2	1.3	1.5	1.6	1.4
72	3.6	3.0	2.7	2.0	2.0	1.7	1.7	1.9	2.1	2.4	2.6	2.9	2.5

Table 2a. RMS error of geopotential height at 500 hPa against analysis (in m)

Hours	Jan	Feb	Mar	Apr	May	Jun	Jul	Aug	Sep	Oct	Nov	Dec	Average
24	10.0	9.9	8.5	8.4	9.4	9.5	11.1	10.0	9.5	10.7	8.9	9.7	9.6
72	20.5	17.7	15.4	14.4	15.9	14.1	15.1	15.0	15.4	17.0	14.2	17.6	16.0

Table 2b. RMS error of geopotential height at 500 hPa against observations (in m)

Hours	Jan	Feb	Mar	Apr	May	Jun	Jul	Aug	Sep	Oct	Nov	Dec	Average
24	14.0	13.9	12.1	12.2	11.4	9.8	9.8	9.6	9.8	12.7	12.4	13.4	11.9
72	27.5	21.7	19.1	17.7	18.9	15.7	16.0	15.3	18.5	19.7	18.7	22.4	19.6

Table 3a. RMS error of vector wind at 850 hPa against analysis (in m/s)

Hours	Jan	Feb	Mar	Apr	May	Jun	Jul	Aug	Sep	Oct	Nov	Dec	Average
24	3.2	3.3	3.1	3.3	3.2	3.2	3.3	3.5	3.7	3.5	3.4	3.4	3.3
72	5.1	5.0	4.8	4.7	4.7	4.7	5.2	5.7	5.8	5.7	4.9	4.9	5.1

Table 3b. RMS error of vector wind at 850 hPa against observations (in m/s)

Hours	Jan	Feb	Mar	Apr	May	Jun	Jul	Aug	Sep	Oct	Nov	Dec	Average
24	4.6	4.6	4.2	4.6	4.4	4.5	4.1	4.0	4.3	4.3	4.4	4.3	4.4
72	6.1	6.0	5.6	5.7	5.7	5.5	5.2	5.2	5.6	5.6	5.7	5.5	5.6

Table 4a. RMS error of vector wind at 250 hPa against analysis (in m/s)

Hours	Jan	Feb	Mar	Apr	May	Jun	Jul	Aug	Sep	Oct	Nov	Dec	Average
24	6.0	5.6	6.2	6.5	6.3	6.1	5.7	5.8	6.4	5.7	5.0	5.1	5.9
72	10.0	8.8	10.1	9.8	10.8	10.1	9.2	8.4	9.4	8.9	8.0	7.8	9.3

Table 4b. RMS error of vector wind at 250 hPa against observation (in m/s)

Hours	Jan	Feb	Mar	Apr	May	Jun	Jul	Aug	Sep	Oct	Nov	Dec	Average
24	10.6	9.8	9.6	9.6	8.2	8.1	6.3	6.1	7.4	7.3	8.5	9.2	8.5
72	12.0	11.6	11.8	11.8	11.6	10.9	9.2	8.5	10.6	9.6	10.2	10.2	10.7

Table 5a. RMS error of temperature at 850 hPa against analysis (in degree Celsius)

Hours	Jan	Feb	Mar	Apr	May	Jun	Jul	Aug	Sep	Oct	Nov	Dec	Average
24	1.6	1.5	1.4	1.2	1.2	1.0	1.1	1.1	1.0	1.2	1.6	1.6	1.3
72	2.9	2.6	2.4	1.7	1.8	1.5	1.5	1.4	1.5	1.9	2.3	2.5	2.0

Table 5b. RMS error of temperature at 850 hPa against observation (in degree Celsius)

Hours	Jan	Feb	Mar	Apr	May	Jun	Jul	Aug	Sep	Oct	Nov	Dec	Average
24	1.6	1.6	1.6	1.5	1.4	1.2	1.3	1.3	1.2	1.6	1.8	1.7	1.5
72	2.4	2.1	2.2	1.9	1.8	1.5	1.4	1.6	1.6	2.0	2.1	2.2	1.9

Table 6a. RMS error of relative humidity at 850 hPa against analysis (in %)

Hours	Jan	Feb	Mar	Apr	May	Jun	Jul	Aug	Sep	Oct	Nov	Dec	Average
24	14.1	14.6	13.8	13.2	12.0	11.4	13.1	13.0	13.2	14.6	16.9	16.4	13.8
72	20.6	20.7	20.0	17.9	18.0	15.7	16.3	16.9	17.2	19.3	23.3	23.0	19.1

Table 6b. RMS error of relative humidity at 850 hPa against observation (in %)

Hours	Jan	Feb	Mar	Apr	May	Jun	Jul	Aug	Sep	Oct	Nov	Dec	Average
24	12.0	12.3	12.9	12.7	11.9	12.3	12.5	12.5	12.7	12.6	13.1	13.2	12.6
72	12.9	13.5	14.2	13.8	13.3	13.7	13.6	13.5	13.2	13.7	13.9	14.2	13.6

Figure 1. RMS error of mean sea level pressure (in hPa) against analysis (solid lines) and observations (dotted lines) at selected forecast hours.

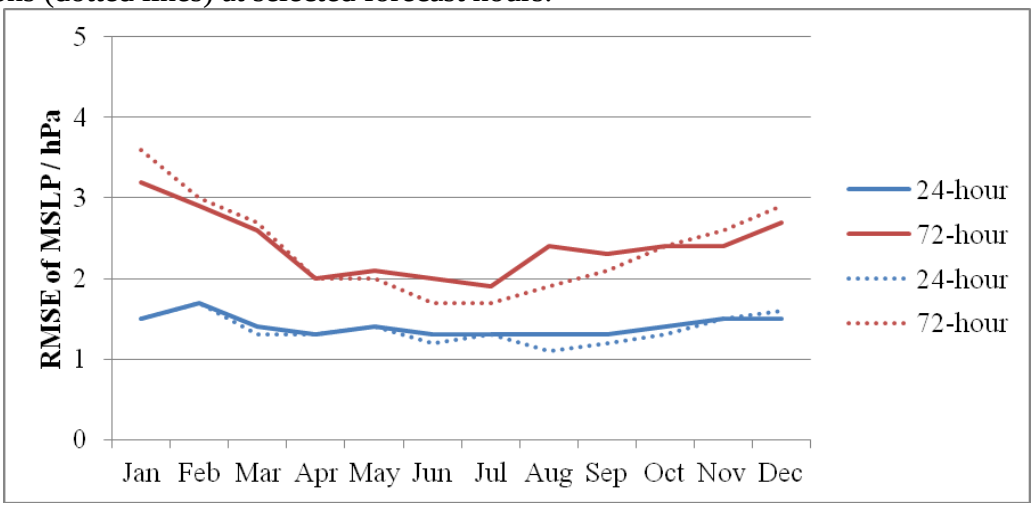

Figure 2. RMS error of geopotential height at 500 hPa (in m) against analysis (solid lines) and observations (dotted lines) at selected forecast hours.

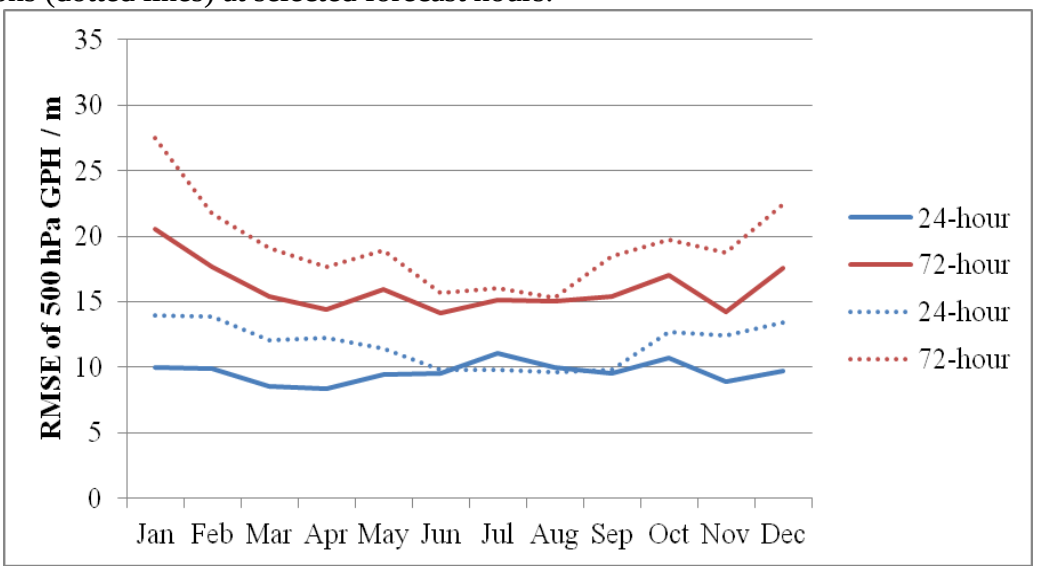

Figure 3. RMS error of vector wind at 850 hPa (in m/s) against analysis (solid lines) and observations (dotted lines) at selected forecast hours.

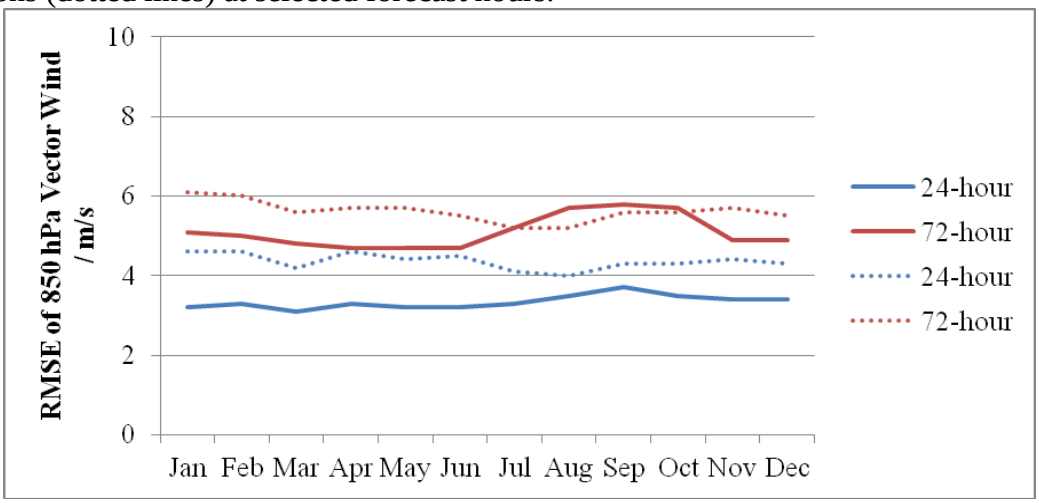

Figure 4. RMS error of vector wind at 250 hPa (in m/s) against analysis (solid lines) and observations (dotted lines) at selected forecast hours.

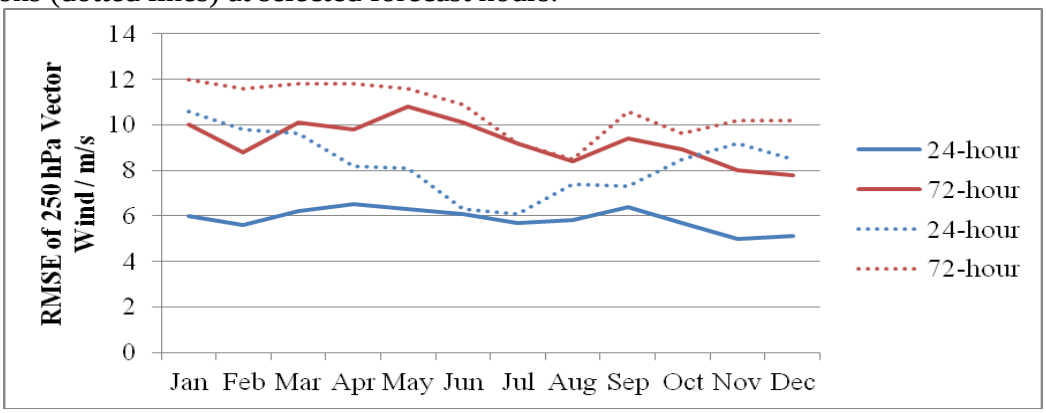

Figure 5. RMS error of temperature at 850 hPa (in degree Celsius) against analysis (solid lines) and observations (dotted lines) at selected forecast hours.

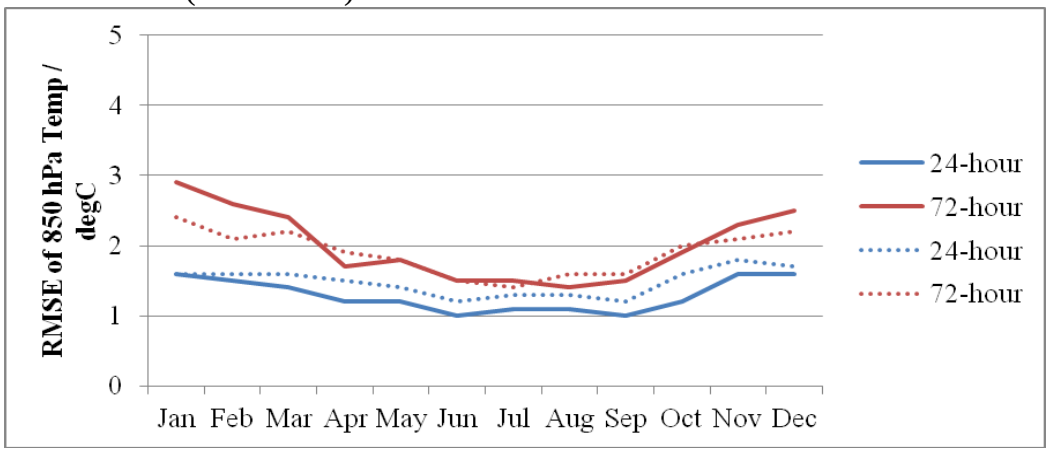

Figure 6. RMS error of relative humidity at 850 hPa (in %) against analysis (solid lines) and observations (dotted lines) at selected forecast hours.

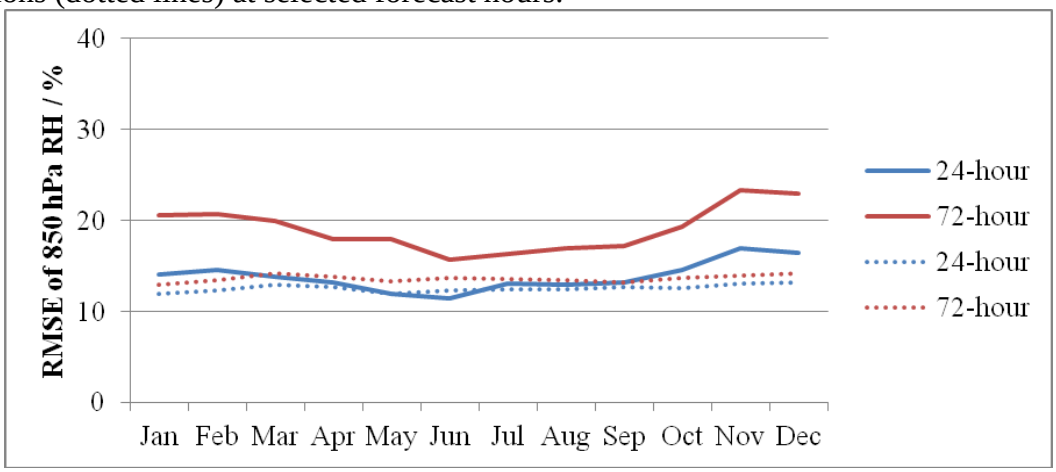

Appendix II – Summary of Verification of Prognostic Products Generated by SLOSH for 2016

Tropical cyclone	Year and Month	Observed maximum storm surge/sea level at Quarry Bay (m)	Predicted maximum storm surge/sea level at Quarry Bay (m)	SLOSH error (observed – Predicted storm surge/sea level (m)
TD	2016 May	0.27/2.35	0.21/2.44	0.06/-0.09
Nida	2016 Aug	0.58/2.93	0.70/1.81	-0.12/1.12
Dianmu	2016 Aug	0.25/2.54	0.21/2.21	0.04/0.33
Sarika	2016 Oct	0.43/2.74	0.27/2.21	0.16/0.53
Haima	2016 Oct	0.54/2.74	0.30/2.30	0.24/0.44

Appendix III – Summary of Verification of Prognostic Products Generated by WAVEWATCH III
00 UTC and 12 UTC Runs for 2016

RMS error of 24-hour significant wave height forecast against observations (in m)

Jan-Mar	Apr-Jun	Jul-Sep	Oct-Dec	Year
1.4 (4262)	1.2 (3229)	0.9 (3229)	1.5 (4799)	1.3 (15519)

(Number of ship reports in brackets)